Eur. J. Biochem. **271**, 2272–2279 (2004) © FEBS 2004 doi:10.1111/j.1432-1033.2004.04170.x

Kinetic studies and molecular modelling attribute a crucial role in the specificity and stereoselectivity of penicillin acylase to the pair ArgA145-ArgB263

Maya Guncheva[1], Ivaylo Ivanov[2], Boris Galunsky[3], Nicolina Stambolieva[1] and Jose Kaneti[1]

[1]*Institute of Organic Chemistry with Centre of Phytochemistry, Bulgarian Academy of Sciences, Sofia, Bulgaria;* [2]*Laboratory of Bioorganic Synthesis, Faculty of Biology, University of Sofia, Bulgaria;* [3]*Department of Biotechnology II, Technical University Hamburg-Harburg, Germany*

Kinetic experiments with a substrate series of phenylacetylarylamides reveal that at least one polar group in the amine moiety is required for the proper orientation of the substrate in the large nucleophile-binding subsite of penicillin acylase of *Escherichia coli*. Quantum mechanical molecular modelling of enzyme–substrate interactions in the enzyme active site shows that in the case of substrates lacking local symmetry, the productive binding implies two nonsymmetrical arrangements with respect to the two positively charged guanidinium residues of ArgA145 and ArgB263. This indicates a crucial role of the specified arginine pair in the substrate- and stereoselectivity of penicillin acylase.

Keywords: enzyme kinetics; molecular modelling; nucleophile specificity and stereoselectivity; penicillin acylase.

Penicillin G acylases (PA, EC 3.5.1.11) from different sources have been widely studied because of their application as industrial biocatalysts for hydrolytic and synthetic transformations in the production of semisynthetic β-lactam antibiotics [1,2] and for their possible new uses in synthetic organic chemistry [3–5]. PA has been identified as an N-terminal nucleophile hydrolase following specific catalytic and processing mechanisms [6–8]. During evolution, the catalytic properties of enzymes have been optimized for their function *in vivo*. However, their application as industrial biocatalysts often requires transformations of substrates not encountered in nature under reaction conditions differing from physiological ones. Protein design aimed at rational optimization and/or effective screening of enzymes for new transformations requires the study of their specificity with appropriate substrate series. Convenient substrates should also contain sensitive reporter groups for spectrophotometric or fluorimetric detection to facilitate rapid and reliable kinetic measurements.

The acyl specificity of PA is restricted to aromatic molecules and has been investigated mainly with substrates containing phenylacetyl, phenylglycyl, mandelyl, pyridylacetyl or other arylacetyl moieties [9–13]. Our previous studies of PA catalysed transfer reactions with a nonspecific acyl moiety, benzoxazol-2-on-3-yl-acetyl, have shown that the hydrolytic ability of PA for such substrates is drastically decreased, but that its nucleophile specificity is more pronounced and the synthetic capacity is, respectively, increased. In the latter system PA behaves as a typical transferase [14,15]. The nucleophile or S_1' [16] specificity of the most studied PA from *Escherichia coli* has been probed in both hydrolytic and kinetically controlled transfer reactions, but the quantitative data published so far are scarce. Specificity constants for PA catalysed hydrolysis of phenylacetyl derivatives with variable leaving groups such as β-lactam nuclei, amino acids, peptides and nucleosides have been shown to differ up to three orders of magnitude [13,17]. Structural, site-directed mutation and kinetic investigations have identified several active site residues important for the S_1'–P_1' interactions relevant to the catalytic mechanism [18–21]. There are, however, still questions to be answered about the alternatives of interactions in the large nucleophile binding subsite. In the substrate series studied here the phenylacetyl moiety is kept constant and the leaving group structures are confined to arylamines. The expected output is a set of comparative kinetic data, which combined with molecular modelling based on available crystallographic data, could give more detailed information on PA nucleophile binding subsite and the mechanism of transformations with this class of compounds. These data can be used further for rational design of substrates for different purposes, e.g. screening of protein engineered PA for new enzymatic transformations, and analysis of kinetics

Correspondence to N. Stambolieva or J. Kaneti, Institute of Organic Chemistry, 1113 Sofia, Bulgaria. Fax: +359 2 70 02 25, E-mail: nstambol@orgchm.bas.bg, kaneti@orgchm.bas.bg; http://www.orgchm.bas.bg/

Abbreviations: PA, penicillin acylase; PhAc, phenylacetyl moiety; 6APA, 6-aminopenicillanic acid; PG or PhAc-6APA, penicillin G; PhAc-NH_2, phenylacetamide; PhAc-MCA, phenylacetyl-4-methylcoumaryl-7-amide; NIPAB, 2-nitro-5-phenylacetamidobenzoic acid; iso-NIPAB, 2-nitro-4-phenylacetamidobenzoic acid; NIPPA, *N*-(5-nitro-2-pyridyl)-phenylacetamide; PhAc-pNA, phenylacetyl 4-nitroanilide; PhAc-pAB, 4-phenylacetamidobenzoic acid; PhAc-mAB, 3-phenylacetamidobenzoic acid; PhAc-oAB, 2-phenylacetamidobenzoic acid; PhAc-βNA, phenylacetyl 2-naphtylamide.
Enzyme: penicillin acylase (EC 3.5.1.11).

(Received 2 February 2004, revised 29 March 2004, accepted 16 April 2004)

of 'invisible' substrates [22]. The correlation of the kinetic parameters with the nucleophile structure could also allow the design of substrate mimetics for more effective acyl transfer [23].

Materials and methods

Materials

Penicillin acylase from *E. coli* was supplied by Antibiotic® Razgrad (Bulgaria) and was purified by anion-exchange chromatography as described previously [24]. All other reagents were analytical grade from Fluka or Sigma.

Substrates

Penicillin G (PG, PhAc-6APA) was from Sigma. Phenylacetamide was synthesized by drop-wise addition of phenylacetyl chloride to concentrated ammonia. The product precipitates. The other studied substrates were synthesized by acylation of the corresponding arylamines (Table 1) with phenylacetyl chloride. The phenylacetamidobenzoic acids were synthesized in aqueous–organic media under slight excess of NaOH according to the Schotten–Baumann procedure [25]. 2-Nitro-5-phenylacetamidobenzoic acid was prepared as described [26]. The other substrates were obtained in dry organic solvents in the presence of organic base (pyridine, *N*-methylmorpholine). The solvents used for the synthesis of the respective phenylacetyl arylamides were tetrahydrofuran for phenylacetyl-4-nitroanilide, *N*-(5-nitropyridin-2-yl)-phenylacetamide and phenylacetyl-2-naphtylamide; dioxan for phenylacetyl-4-methylcoumaryl-7-amide. Phenylacetyl chloride was added drop-wise into the arylamine solution at 0 °C. Then the reaction mixture was allowed to reach room temperature and the reaction was further carried out at the boiling point of the organic solvent. The products were recrystallized: the phenylacetamidobenzoic acids, phenylacetyl-4-nitroanilide, phenylacetyl-4-methylcoumaryl-7-amide and phenylacetamide from ethanol; *N*-(5-nitropyridin-2-yl)-phenylacetamide from $CHCl_3$/hexane; phenylacetyl-2-naphtylamide from acetone/petroleum ether. The yields varied in the range 60–90%. The synthesized substances were identified by their melting point, elemental analysis and ^{1}H-NMR spectra. In the case of phenylacetamido-benzoic acids and phenylacetyl-4-methylcoumaryl-7-amide the melting points are in good agreement with previously published data [27,28]. The newly synthesized *N*-(5-nitropyridin-2-yl)-phenylacetamide has a melting point of 145–146 °C;

Table 1. Phenylacetyl arylamides used as probes for the nucleophile binding subsite of *E. coli* PA.

Substrate (abbreviation)	Structure of the leaving amine	Method to trace the course of the reaction
1 NIPAB	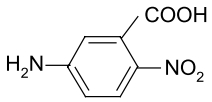	Spectrophotometric $\lambda = 380$ nm, $\varepsilon = 11600$ м$^{-1}$·cm^{-1}
2 PhAc-MCA	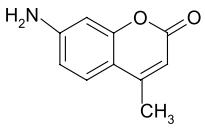	Spectrofluorimetric $\lambda_{ex} = 380$ nm, $\lambda_{em} = 460$ nm
3 PhAc-*p*NA	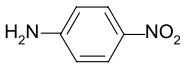	Spectrophotometric $\lambda = 410$ nm, $\varepsilon = 7900$ м$^{-1}$·cm^{-1}
4 NIPPA	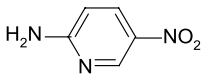	Spectrophotometric $\lambda = 370$ nm, $\varepsilon = 11200$ м$^{-1}$·cm^{-1}
5 PhAc-*p*AB	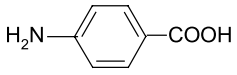	Spectrophotometric $\lambda = 295$ nm, $\varepsilon = 6450$ м$^{-1}$·cm^{-1}; Discontinuous colour assay
6 PhAc-βNA	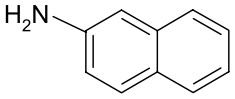	Spectrofluorimetric $\lambda_{ex} = 335$ nm, $\lambda_{em} = 420$ nm
7 PhAc-*m*AB	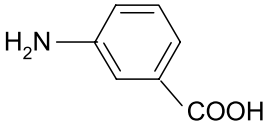	Discontinuous colour assay
8 PhAc-*o*AB	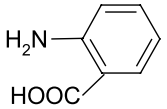	Spectrofluorimetric $\lambda_{ex} = 340$ nm, $\lambda_{em} = 420$ nm; Spectrophotometric $\lambda = 325$ nm, $\varepsilon = 3500$ м$^{-1}$·cm^{-1}

calculated for $C_{18}H_{11}N_3O_3$: C 60.70, H 4.31, N 16.33, found: C 60.83, H 4.58, N 16.18; ^{1}H NMR: 3.81 (s, 2H, C_6H_5-CH_2), 7.21–7.36 (m, 5H, C_6H_5), 8.24–9.18 (m, 3H, Pyr-H), 11.46 (s, 1H, *NH*CO).

Kinetic measurements

The PA-catalysed hydrolysis of the arylamide bond was followed by the absorbance or fluorescence change during the release of the product (see Table 1 for the corresponding spectral characteristics). The hydrolysis of 3-phenylacetamidobenzoic acid (PhAc-*m*AB) and 4-phenylacetamidobenzoic acid (PhAc-*p*AB) was followed by a discontinuous colour assay, based on the diazotization-coupling method [29]. The hydrolysis of the reference substrates phenylacetamide ($PhAcNH_2$) and PhAc-6APA was followed by HPLC as described earlier [13]. The kinetic experiments were performed at 25 °C in 50 mM phosphate buffer pH 7.0, containing 10% dimethyl sulfoxide. The concentration range of each substrate was based on its solubility and typically was 20–300 μM. For steady-state kinetic analysis of substrates of high K_m values this range was not always the most appropriate. For such cases the specificity constants k_{cat}/K_m were determined from pseudo-first order traces. The enzyme concentration was in the range 50–100 nM, determined by active site titration [30] using 2-nitro-5-phenylacetamidobenzoic acid (NIPAB) as a substrate. The steady-state kinetic parameters were derived from the initial rates for at least seven different substrate concentrations using the nonlinear regression data analysis software ENZFITTER [31].

Modelling and analysis of interaction energies within the active site

Initial graphic visualization and manipulation of molecules were performed using the program DS VIEWERPRO (Accelrys Corporation, San Diego, CA, USA; http://www.accelrys.com/dstudio/ds_viewer/index.html). Models were based on the crystallographic coordinates of the enzyme–substrate complex AsnB241Ala mutant *E. coli* PA with PG [19] (Brookhaven Protein Data Bank [32], entry number 1fxv). Approximate docking of an Asn residue in place of Ala as in the native enzyme in this structure was performed using the SWISS-PDB VIEWER program [33] (http://www.expasy.ch/spdbv/mainpage.htm). The atoms of the phenylacetyl group were arranged close to the position found in the complex with PG [19]. The bond lengths and valence angles of the nitroaniline moiety were taken from the X-ray data for the system cyclophilin A and the tripeptide substrate succinyl-Ala-Pro-Ala-*p*-nitroanilide [34].

The structures of enzyme–substrate complexes with docked substrates were refined by another procedure. First, we chose a selection of limited number of amino acid (oligopeptide) residues in the immediate vicinity of the substrate in order to estimate the contribution of each protein fragment to the interaction energy of the complex. Then, the resulting 'supermolecule' was subjected to explicit optimization of the position of substrate within the 'truncated active site'. In this step, coordinates of all amino acid or oligopeptide fragments were kept frozen at their values from the X-ray structure, while all coordinates of substrate atoms were optimized using AM1 semiempirical MO calculations [35] as implemented in the MOPAC 93 program package [36]. This procedure as such has two caveats. First, the assumption of fixed amino acid positions is equivalent to freezing the enzyme process to a time point at which substrate binding is complete, and the catalytic act has not started yet. This moment is convenient from the viewpoint of required computing power. Second, and more important, is that the optimization of substrate position within the catalytic cavity of PA encounters multiple energy minima. Therefore, the way the best of these, i.e. the global minimum, was chosen 'automatically' was crucial. We used the eigenvector-following optimization [37] with stringent convergence criteria and unconstrained geometry search. Thus, we expected the search method to skip shallow local minima on the respective potential energy surface, and hoped to gain some enhanced probability to achieve a significantly populated minimum. This is essentially another docking procedure, using semiempirical AM1 quantum mechanical calculations.

The final, more precisely docked structures, were visualized using MOLEKEL [38]. The interaction energies within the optimized complex and their decomposition into Coulombic, polarization, charge transfer and exchange repulsion components were analysed using the procedure of Morokuma [39] at the RHF STO-3G level of MO theory [40], as implemented in the GAMESS-US computational package [41]. The modelling process was performed for a selection of amino acid residues within the active site consisting of 10 fragments, including the substrate, and comprising a total of 298–312 atoms depending on substrate size.

Results and discussion

Substrate structure and kinetic results

We selected the leaving groups in the studied phenyacetyl arylamides considering both steric and electronic factors. The structures listed in Table 1 are of different size and hydrophobicity, without and with electronegative substituents of different orientation, and the majority possesses chromogenic or fluorogenic properties. The kinetic parameters of the PA-catalysed hydrolysis of the studied phenylacetyl arylamides are compared in Table 2. The substrates are arranged in a decreasing order of the ratio of their specificity constant to the specificity constant of phenylacetamide (PhAc-NH_2), used as a reference because it implies no interactions in the large S_1' binding subsite. NIPAB has a specificity constant of the same order of magnitude as one of the most specific substrate of PA–PG. Phenylacetyl-4-methylcoumaryl-7-amide (PhAc-MCA) has a specificity constant almost equal to that of the reference substrate. The remaining PhAc-arylamides have 5–50 times lower specificity constants. Thus, specificity constants for the best (NIPAB) and the worst (2-phenylacetamidobenzoic acid; PhAc-*o*AB) substrates in this series differ by more than two orders of magnitude, which reflects the sensitivity of the enzyme towards the structural changes in the leaving arylamine moiety. These changes account for differences in K_m and k_{cat}, which implies that S_1'–P_1' interactions, both in the ground and transition states, are important for the catalytic efficiency of PA with the studied substrates.

Table 2. Steady-state kinetic data for PA catalysed hydrolysis of phenylacetyl arylamides with different leaving groups. Reaction conditions: 25 °C, 50 mM phosphate buffer pH 7.0, 10% dimethyl sulfoxide. The SD from the mean value was < 10% in three determinations. Substrate numbering is the same as in Table 1.

	Substrate	k_{cat} (s^{-1})	$10^6 \times K_m$ (M)	$10^{-5} \times k_{cat}/K_m$ ($M^{-1} \cdot s^{-1}$)	Ratio to reference PhAc-NH_2
	PhAc-6APA[a]	50	10	50	20
1	NIPAB	20	15	13.3	5.3
	iso-NIPAB[b]	100	80	12.5	5.2
2	PhAc-MCA	3.2	12	2.7	1.1
	PhAc-NH_2[a]	50	200	2.5	1.0
3	PhAc-*p*NA[c]	20	400	0.5	0.2
4	NIPPA	7.8	510	0.15	0.06
5	PhAc-*p*AB	3.0	300	0.1	0.04
6	PhAc-βNA	1.9	200	0.095	0.039
7	PhAc-*m*AB	2.5	400	0.06	0.024
8	PhAc-*o*AB	2.3	630	0.04	0.016

[a] The kinetic constants for PA catalysed hydrolysis of PG and PhAc-NH_2 are determined at the same reaction conditions and are used as reference values. [b] Data for iso-NIPAB from Ref [42]. [c] Literature data for this substrate: k_{cat} 50 s^{-1}, K_m 120 μM at 25 °C in10 mM phosphate buffer pH 7.5, 0.1 M KCl [42]; k_{cat} 14 s^{-1}, K_m 130 μM) at 30 °C in 50 mM phosphate buffer pH 7.0 [43].

The proper orientation of COOH and NO_2 substituents in the aminoaryl moiety favours the hydrolytic reaction of NIPAB. PhAc-arylamides with only one (NO_2 or COOH) substituent are substantially worse substrates. The data for the PA catalysed hydrolysis of PhAc-Asp and PhAc-Glu [13] and our data for PhAc-*p*AB, PhAc-*m*AB and PhAc-*o*AB (Table 2) imply that the COOH group has to be positioned as in NIPAB for effective catalysis. The incorporated pyridyl moiety in *N*-(5-nitro-2-pyridyl)-phenylacetamide (NIPPA) might lead to alternative interactions within the active site, resulting in different orientation and binding.

Molecular modelling

The X-ray structures of PA (wild-type and mutant) complexes with different ligands [19,20,44,45] indicate the presence of a single roughly conical groove, the hydrophobic part of which accommodates the phenylacetyl moiety of the ligands. The more polar aminic moiety resides in the open part of the groove, surrounded by several polar amino acid residues. This part of the enzyme can be considered as its S_1' binding subsite. Substrate binding induces conformational changes involving the ArgA145-PheA146 fragment of the protein chain, acting as a flap, first opening and then closing the groove [45]. The catalytic reaction presumably occurs when the ionized carboxyl group of PG approaches the guanidine side chain of ArgA145, thereby turning the scissile amide bond inside the groove towards SerB1. SerB1 is involved in the hydrogen bond network around ArgB263 and AsnB241 (Fig. 1). Hydrogen bonds observed in the free PA (PDB ID: 1pnk) are believed to maintain the appropriate three-dimensional

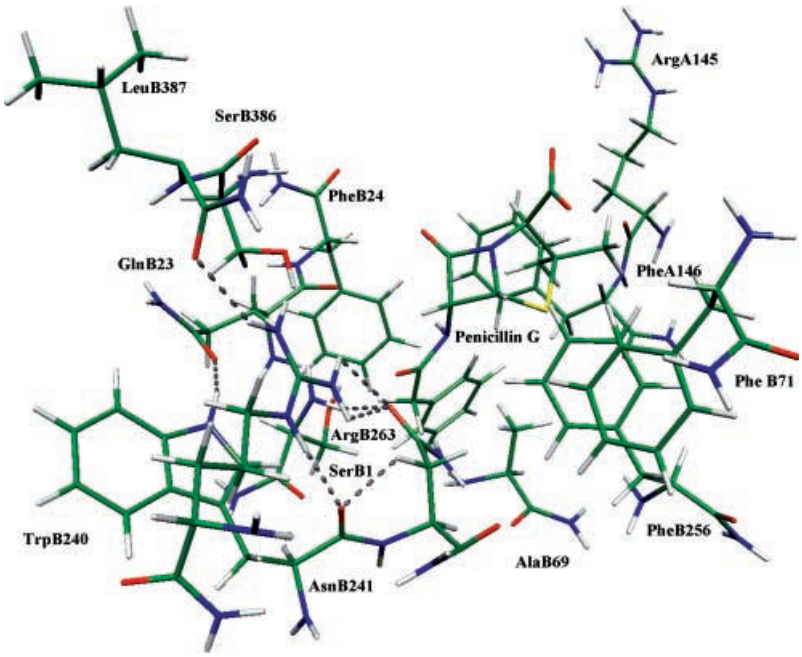

Fig. 1. The hydrogen bond network (broken lines) around ArgB263 as derived from X-ray coordinates of amino acid residues in penicillin acylase [19] and AM1 docking calculations. The three N atoms of the side chain δ-guanidino group of this residue are involved in H-bonding as follows: Nε with the O atom of the main chain CO group of the TrpB240; $N\eta^1$ shares H bonding with O atom of the CO group of LeuB387 together with O atom of γ-OH of SerB386; $N\eta^2$ is in H bonding with $O\delta^1$ of AsnB241. In the free enzyme, a bridging water molecule W360 bonded with γ-OH of SerB386 and $N\eta^2$ of ArgB263, respectively, closes the H-bond network. Atom colours used are: C, green; N, blue; O, red; S, yellow.

arrangement of catalytically essential amino acid residues [44,46]. The same H-bond network is evidenced also in the complexes of wild-type PA with phenylacetic acid and PG sulphoxide (PDB ID: 1pnl and 1g7) and in the complex of Asn241Ala mutant with PG (PDB ID: 1fxv) [19,20,45]. With the exception of a recent publication [47], ArgB263 has not been discussed as a residue potentially involved in S_1'–P_1' interactions. ArgB263 is fully conserved in 11 PA sequences (CLUSTALW alignment; http://www.ebi.ac.uk/clustalw) and can be assigned the role of 'main coordinator' of the catalytic hydrogen bond network. This implies that the ArgB263 residue could be involved both in catalysis and productive binding.

Graphic simulation of the interactions of arylamide substrates with the nucleophile binding subsite of PA indicates that the arylamide moiety is accessible by solvent. Along with the suggestion of a large volume ($\approx$ 1000 Å^3) of this subsite [48], it implies relatively weak interactions between the leaving group and the selected polar amino acid residues. This is in good agreement with the K_m values for PhAc-NH_2 (200 μM) and PhAc-OMe (160 μM) [46], both substrates practically lacking S_1'–P_1' interactions, and with the K_m values (200–600 μM) for the majority of the studied PhAc-arylamides more than one order of magnitude higher than the corresponding value of PG. The same deduction is also well in line with the diversity of the tolerated P_1' structures by PA. The situation significantly changes for NIPAB hydrolysis, where a negatively charged substituent is present in the *m*-position, along with a polar one in the *p*-position to the scissile amide bond. Modelling of the possible hydrogen bond network around ArgB263 accommodating the polar leaving group of NIPAB accounts for significant electrostatic interactions between polar amino acid residues and the latter substrate (Fig. 2, bottom left). A similar, although less hydrogen bonded, arrangement of NIPAB is possible with ArgA145, with or without the participation of bridging water molecules. In the model complex with NIPAB, the phenylacetyl moiety of this substrate is placed in the close vicinity of the catalytic SerB1 and AsnB241 from the oxyanion hole, essential for stabilization of the tetrahedral intermediate. Experimental data [21] for the efficient hydrolysis of NIPAB catalysed by the ArgB263Lys mutant PA and the lack of hydrolytic activity for the ArgB263Leu PA mutant (K_m value increased 15-fold) also imply that this residue participates in the productive binding of NIPAB. However, Alkema *et al.* [21] reject this role of ArgB263 and propose TyrB31 as a possible basic residue interacting with this substrate. Their conclusion is based on pH dependence studies and the observed pK_a value of $\approx$ 9, considered too low for guanidino group (pK_a 12.5). Indeed, it is hard to assume such an alteration in the polar environment of this side chain. It is formed by the

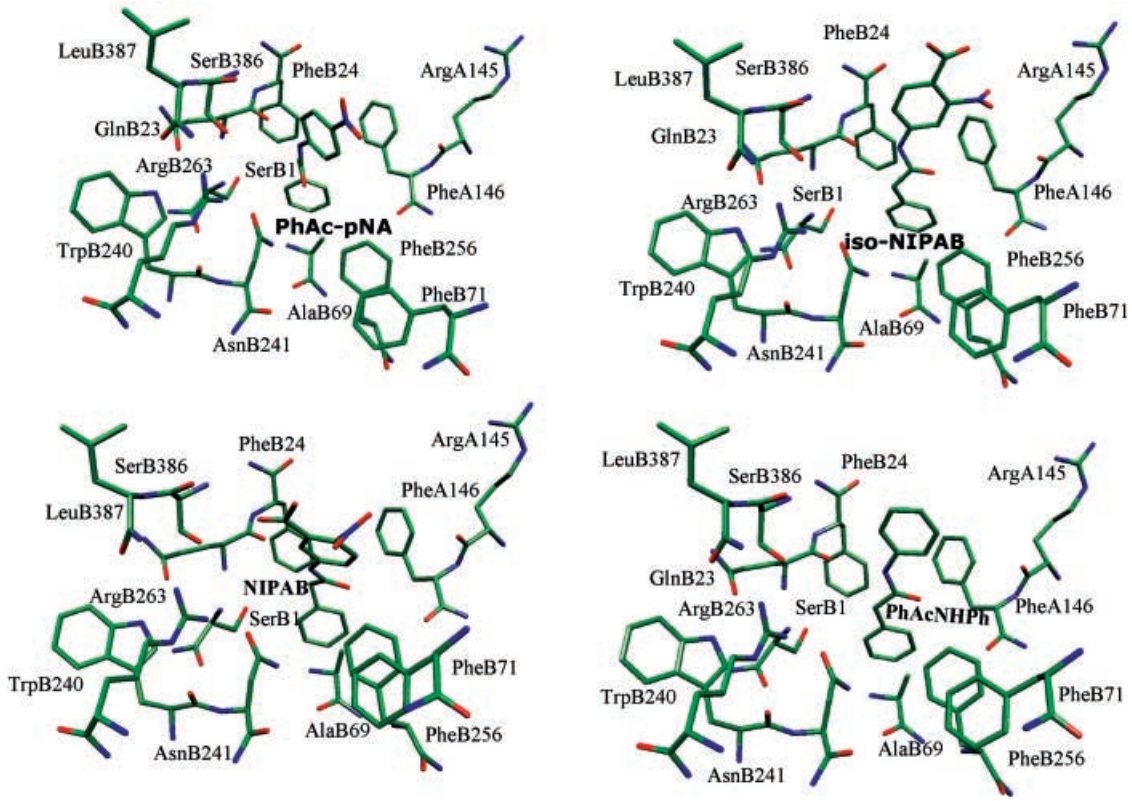

Fig. 2. The optimized positions of some arylamide substrates docked in the active site of penicillin acylase by AM1 calculations. Amino acid residues of the enzyme are at their X-ray coordinates [19]. Substrates having local symmetry of the leaving group (top left and bottom right) bind at an equilibrium point of the electrostatic action of the two guanidinium residues. Substrates with leaving groups lacking local symmetry (for NIPAB, bottom left, COO^- is close to ArgB263; for iso-NIPAB, top right, NO_2 is close to ArgA145) can assume either of the two directions depending on the orientation of the polar group.

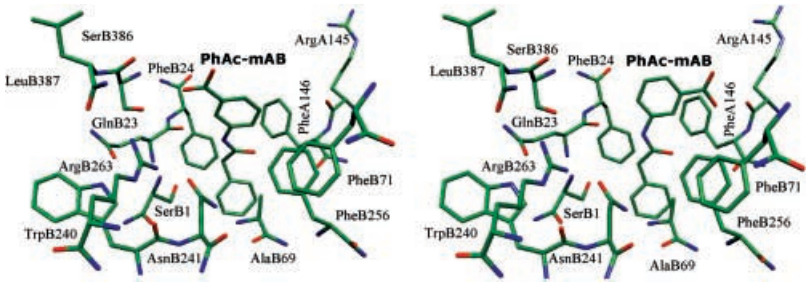

Fig. 3. Penicillin acylase stereoselection of achiral arylamide substrate with a leaving group lacking local symmetry. The simultaneous strong electrostatic action of the two positively charged residues, ArgA145 and ArgB263, on the negatively charged COO^- in the aminic part determines the position of the substrate within the S_1'-binding subsite.

O atoms of the main chain CO groups of LeuB387 and TrpB240, Oδ[1] atom of AsnB241, and Oγ atom of SerB386 and is expected to stabilize the positive charge of ArgB263. All of these views remain arguable, but one should always be careful when addressing experimental macroscopic pK_a values to a specified functional group in an enzyme molecule, as shown by Carpenter and Fersht [49,50].

Considerations of the suggested hydrogen bond network around ArgB263 provide no reasonable explanation of the PA activity with substrates like PhAc-*p*AB, PhAc-*m*AB, PhAc-*o*AB vs. phenylacetyl 4-nitroanilide (PhAc-*p*NA), NIPAB and iso-NIPAB, but it suggests an explanation of the 16-fold difference between the K_m values of PhAc-MCA and PhAc-βNA (Table 2). The determined lower K_m value for the PhAc-MCA could be ascribed to a more favourable hydrogen bonding interaction between ArgB263 and the remote carbonyl group of MCA, which interaction is absent with the βNA moiety.

The analysis of differences observed between the k_{cat} values for the studied PhAc-arylamides is more complex. On one hand, structural data for the PA–substrate interactions in the transition state are missing and only a GRID computational modelling approach to the tetrahedral intermediate in PA presents some indications of the importance of ArgB263 for enzyme–substrate interactions [48]. On the other hand, the determined catalytic constants are apparent ones, with varying relative contributions of individual rate constants and their discussion is not straightforward.

An important detail of the modelling experiments with possible arrangements of substrates within the X-ray structure of PA requires special attention. One should note that substrates bearing aminic moieties without local symmetry can adopt at least two spatially different alignments within the active site. This should be particularly true for substrates having polar substituents, e.g. NIPAB (Fig. 2, bottom left) with the carboxylate group directed towards ArgB263. The possible alternative orientation of NIPAB in the S_1' binding subsite towards ArgA145 (analogously to Fig. 3, right) follows the mode of binding of PG in the complex with AsnB241Ala mutant PA [19]. This three-dimensional difference in substrate arrangements within the PA active site certainly has to do with the stereoselectivity of this enzyme.

Quantum mechanical molecular modelling

AM1 optimization of substrate position and conformation within our selection of PA active site fragments places NIPAB somewhat closer to ArgB263 than to ArgA145. The distances between the polar CO_2^- and O(NO) and positively charged guanidinium fragments of ArgA145 and ArgB263 are listed in Table 3. AM1 docking calculations show uniformly that PG and phenylacetyl arylamides have the benzyl fragment $PhCH_2$ placed in the hydrophobic groove of the active site. The polar fragments of all substrates align between the positively charged ArgA145 and ArgB263, with the carboxyl group of PG somewhat closer to ArgA145, while nitroarylamides have the polar NO_2 at roughly equal distances from the two guanidinium fragments. More important, the COO^- groups of arylamides on Figs 2 and 3 are at approximately equal distances from the two positively charged fragments as well, Table 3. The complexes of selected phenylacetyl arylamides with the mentioned selection of amino acid and oligopeptide residues from the active site of PA are shown on Figs 1,2 and 3.

Table 3. Distances (Å) between polar substrates groups (CO_2^- and NO_2) and the two ArgB263 and ArgA145 residues of penicillin acylase as a result of AM1 optimization of the corresponding substrate position in the selected PA fragment environment.

	NIPAB		PG	PG sulfoxide
Arg residue	O(CO)-N[a]	O(NO)-N[a]	O(CO)-N[a]	O(CO)-N[a]
ArgA145	9.8	10.2	8.2	12.1
ArgB263	6.6	6.7	8.7	6.7

[a] N is one of the nitrogen atoms of the corresponding guanidino group.

The AM1 docked complex of PG is shown on Fig. 1. The discussed hydrogen bond network around ArgB263 is retained also with arylamide substrates and involves their polar carboxylate and/or nitro groups. For substrates with leaving groups, lacking local symmetry, e.g. NIPAB, PG, as well as with the poor substrate PhAc-mAB, we were able to model complexes with the mentioned selection of amino acid residues around the catalytic site of PA, having the COOH group directed to either ArgA145, or ArgB263 (Fig. 3). These results emphasize the caveat of multiple minima for the accommodation of substrate within the active site of PA. More importantly, however, the possibility of polar group orientation towards either ArgA145 or ArgB263 indicates a source of substrate specificity and stereoselectivity of PA at the molecular level. Experimental observations on the pH dependence of PA enantioselectivity [51] coincides well with the above conclusions. Computational modelling of PA enantioselectivity in the reverse reaction of amide bond synthesis also has pointed at the role of ArgB263 in this process [48].

The decomposition of interaction energies within the studied complexes, shown in Table 4, indicates relatively

Table 4. Calculated STO−3G interaction energies (kcal·mol^{-1}) for various substrates with the larger 10-fragment selection of protein residues within the active site of penicillin acylase. Superscripts at total energies indicate the direction of nonsymmetrical polar groups towards either ArgA145 or ArgB263. Partial energy contributions from the two arginine residues and the substrate are given vs. measured K_m values given in Table 2.

Substrate	$E_{I\ total}$	$E_{ArgA145}$	$E_{ArgB263}$	$E_{Substrate}$	$10^6 \times K_m$ (M)
PG					10
NIPAB	-60.4^{145}	−0.5	−4.2	−3.7	15
iso-NIPAB	-61.3^{145}	−0.6	−4.0	−3.6	80
	-121.5^{263}	−0.4	−4.2	−3.7	
PhAc-*m*AB	-61.7^{145}	−2.4	−4.0	−4.4	400
	-63.4^{263}	−0.2	−3.9	−7.4	
PhAc-*p*NA	−56.4	−0.5	−4.1	−23.3	400
PhAcNHPh	−55.9	−0.3	−4.0	−5.8	

smaller contributions of ArgA145 to individual terms of the interactions: electrostatic, charge transfer, and polarization. On the contrary, contributions from ArgB263 are significantly larger and generally comparable to those of the nucleophile SerB1, GlnB23-PheB24, AlaB69, believed to be the dominant substrate binding fragments of PA. In addition, substrates with leaving groups lacking local symmetry may have their polar group directed towards ArgB263. In this case calculated interaction energies with the rest of the complex are larger than in the case of substrates with the polar group oriented towards ArgA145. The interaction energy of ArgA145 itself with the rest of the complex is large when the substrate's polar group is directed toward it, and small when the polar group points to ArgB263. The interaction energy of ArgB263 with the rest of the complex, however, remains large and practically constant irrespective of the orientation of the polar group. While a significant part of the latter relatively large interaction energy can be attributed to the hydrogen bonding network around ArgB263, the mentioned findings give another argument favouring the importance of ArgB263 in substrate binding to PA. The pronounced difference in interaction energies of the two arginine residues shows certain capability of the pair of polar guanidinium groups to discern between orientations of substrates in the active site. These two arginines should thus contribute significantly to enzyme stereoselectivity. A more detailed account of the Morokuma analysis [39] of interaction energies in PA active site complexes will be given elsewhere (J. Kaneti, S. Bakalova, I. Ivanov, M. Guncheva & N. Stambolieva, unpublished data).

Conclusions

Kinetic and molecular modelling studies with a substrate series of phenylacetyl arylamides reveal that at least one polar group in the amine moiety of the substrate is essential for its proper orientation in the large nucleophile binding subsite of penicillin acylase.

AM1 docking calculations based on the crystal structure [19] give evidence of polar environment around ArgB263. It consists of O atoms of the main chain CO groups of LeuB387 and TrpB240, Oδ^1 atom of AsnB241 and Oγ atom of SerB386 and is expected to stabilize the positive charge of ArgB263.

The possible nonsymmetrical accommodation of substrates with respect to the pair of ArgA145 and ArgB263 of PA gives rise to notable three-dimensional stereochemical differences in their corresponding enzyme–substrate complexes, and to a certain degree of stereoselectivity. The pair ArgA145 and ArgB263 significantly influences the S_1' specificity and contributes to the appropriate docking of the substrate.

References

1. Bruggink, A., Ross, E.C. & de Vroom, E. (1998) Penicillin acylase in the industrial production of β-lactam antibiotics. *Org. Process Res. Devel.* **2**, 128–133.
2. Bruggink, A., ed. (2001) *Synthesis of β-Lactam Antibiotics. Chemistry, Biocatalysis and Process Integration.* Kluwer Academic Publishers, Dordrecht, the Netherlands.
3. Didziapetris, R., Drabing, B., Schellenberger, V., Jakubke, H.-D. & Svedas, V. (1991) Penicillin acylase-catalysed protection and deprotection of amino groups as a promising approach in enzymatic peptide synthesis. *FEBS Lett.* **287**, 31–33.
4. Waldmann, H., Heuser, A. & Reidel, A. (1994) Selective enzymatic deprotection of hydroxy and amino groups in carbohydrates and nucleosides. *Synlett* 65–67.
5. Sheldon, R.A., van Rantwijk, F., van Langen, L.M., Wegman, M.A., Cao, L. & Janssen, M.H.A. (2001) Biocatalysis and biocatalyst in the synthesis of β-lactam antibiotics. In: *Synthesis of β-Lactam Antibiotics. Chemistry, Biocatalysis and Process Integration* (Brugging, A., ed.), pp. 137–143. Kluwer Academic Publishers, Dordrecht, the Netherlands.
6. Brannigan, J.A., Dodson, G., Duggleby, H.J., Moody, P.C., Smith, J.L., Tomchick, D.R. & Murzin, A.G. (1995) A protein catalytic framework with an *N*-terminal nucleophile is capable of self-activation. *Nature* **378**, 416–419.
7. Suresh, C.G., Pundle, A.V., SivaRaman, H., Rao, K.N., Brannigan, J.A., McVey, C.E., Verma, C.S., Dauter, Z., Dodson, E.J. & Dodson, G.G. (1999) Penicillin V acylase crystal structure reveals new *N*tn-hydrolase family members. *Nat. Struct. Biol.* **6**, 414–416.
8. Dodson, G.G. (2000) Catalysis in penicillin G amidase – a member of the *N*tn (*N*-terminal nucleophile) hydrolase family. *Croatica Chemica Acta* **73**, 901–908.
9. Cole, M. (1969) Deacylation of acylamino compounds other than penicillins by the cell-bound penicillin acylase of *E. coli*. *Biochem. J.* **115**, 741–745.
10. Cole, M., Savidge, T. & Vanderhaeghe, H. (1975) Penicillin acylase (Assay). *Methods Enzymol.* **43**, 699–721.
11. Pohl, T. & Waldmann, H. (1995) Enhancement of the enantioselectivity of penicillin G acylase from *E. coli* by 'substrate tuning'. *Tetrahedron Lett.* **36**, 2963–2966.
12. Fuganti, C., Rosell, C.M., Rigoni, R., Servi, S. & Tagliani, A. (1992) Penicillin acylase mediated synthesis of formylcephamandole. *Biotechnol. Lett.* **14**, 543–546.

13. Galunsky, B., Lummer, K. & Kasche, V. (2000) Comparative study of substrate- and stereospecificity of penicillin G amidases from different sources and hybrid isoenzymes. *Chem. Monthly* **131**, 623–632.
14. Stambolieva, N., Mincheva, Z., Galunsky, B. & Kalcheva, V. (1992) Penicillin amidase-catalysed transfer of low specific acyl moiety. Synthesis of 7-benzoxazolonylacetamido-desacetoxy-cephalosporanic acid. *Enzyme Microb. Technol.* **14**, 496–500.
15. Stambolieva, N., Mincheva, Z. & Galunsky, B. (1998) Kinetic Comparison of penicillin amidase-catalysed transfer of nonspecific and specific acyl moieties to 7-ADCA. *Biocat. Biotrans.* **16**, 225–232.
16. Schechter, I. & Berger, A. (1967) On the size of the active site in proteases. I. Papain. *Biochem. Biophys. Res. Commun.* **27**, 157–162.
17. Youshko, M.I., Chilov, G., Scherbakova, T. & Svedas, V.K. (2002) Quantitative characterization of the nucleophile reactivity in penicillin acylase-catalyzed acyl transfer reactions. *Biochim. Biophys. Acta* **1599**, 134–140.
18. Brannigan, J.A., Dodson, G.G., Done, S.H., Hewitt, L., McVey, C.E. & Wilson, K.S. (2000) Structural studies of penicillin acylase. *Appl. Biochem. Biotechnol.* **88**, 313–319.
19. Alkema, W.B.L., Hensgens, C.M.H., Kroezinga, E.H., de Vries, E., Floris, R., van der Laan, J.-M., Dijkstra, B.W. & Janssen, D.B. (2000) Characterization of the β-lactam binding site of penicillin acylase of *E. coli* by structural and site-directed mutagenesis studies. *Protein Eng.* **13**, 857–863.
20. McVey, C.E., Walsh, M.A., Dodson, G.G., Wilson, K.S. & Brannigan, J.A. (2001) Crystal structure of penicillin acylase enzyme-substrate complexes: Structural insights into the catalytic mechanism. *J. Mol. Biol.* **313**, 139–150.
21. Alkema, W.B.L., Prins, A.K., de Vries, E. & Janssen, D.B. (2002) Role of α Arg^{145} and β Arg^{263} in the active site of penicillin acylase of *Escherichia coli*. *Biochem. J.* **365**, 303–309.
22. Alkema, W.B.L., Floris, R. & Janssen, D.B. (1999) The Use of chromogenic reference substrates for the kinetic analysis of penicillin acylases. *Anal. Biochem.* **275**, 47–53.
23. Bordusa, F. (2000) Nonconventional amide bond formation catalysis: programming enzyme specificity with substrate mimetics. *Braz. J. Med. Biol. Res.* **33**, 469–485.
24. Kasche, V., Haufler, U., Markowski, D., Zeich, A. & Galunsky, B. (1987) Penicillin amidase from *E. coli*. Enzyme heterogeneity and stability. *Ann. N.Y. Acad. Sci.* **501**, 97–102.
25. Vogel, A. (1978) *Vogel's Text Book of practical Organic Chemistry*, 4th edn. pp. 672–673. Longman Scientific & Technical, New York, USA.
26. Daumy, G.O., McColl, A.S. & Apostolakis, D. (1982) Repression of penicillin G acylase of *Proteus rettgeri* by tricarboxylic acid cycle intermediates. *J. Bacteriol.* **152**, 104–110.
27. Szewczuk, A., Siewinski, M. & Slowinska, R. (1980) Colorimetric assay of penicillin amidase activity using phenylacetyl-aminobenzoic acid as substrate. *Anal. Biochem.* **103**, 166–169.
28. Schepper, T., Weiss, M. & Schügerl, K. (1986) Two new fluorogenic substrates for detection of penicillin G-acylase activity. *Anal. Chim. Acta* **182**, 203–206.
29. Norwitz, G. & Keliher, P. (1981) Spectrophotometric determination of aniline by the diazotization-coupling method with 8-amino-1-hydroxynaphthalene-3,6-disulfonic acid as the coupling agent. *Anal. Chem.* **53**, 56–60.
30. Svedas, V.K., Margolin, A.L., Sherestyuk, C.F., Klyosov, A.A. & Berezin, I.V. (1977) Phenylmethansulfonylfluoride inactivation of soluble and immobilized penicillin amidase from *E. coli*. Kinetic analysis and titration of active site. *Bioorg. Khim.* **3**, 547–553.
31. Leatherbarrow, R.J. (1987) ENZFITTER. Elsevier Biosoft, Cambridge, UK.
32. Berman, H.M., Westbrook, J., Feng, Z., Gilliland, G., Bhat, T.N., Weissig, H., Shindyalov, I.N. & Bourne, P.E. (2000) The protein data bank. *Nucleic Acids Res.* **28**, 235–242.
33. Guex, N. & Peitsch, M.C. (1997) SWISS-MODEL and the Swiss-PdbViewer: An environment for comparative protein modeling. *Electrophoresis* **18**, 2714–2723.
34. Konno, M., Ito, M., Hayano, T. & Takanashi, N. (1996) The substrate-binding site in *E. coli* cyclophilin A preferably recognizes a cis-proline isomer or a highly distorted form of the trans isomer. *J. Mol. Biol.* **256**, 897–908.
35. Dewar, M.J.S., Zoebisch, E.G., Healy, E.F. & Stewart, J.J.P. (1985) AM1: a new general purpose quantum mechanical molecular model. *J. Am. Chem. Soc.* **107**, 3902–3909.
36. Stewart, J.J.P. (1993) MOPAC 93 & MOPAC 7: Linux Public Domain: http://www.webmo.net/download/mopac7.tar.z
37. Baker, J. (1986) An algorithm for the location of transition states. *J. Comput. Chem.* **7**, 385–395.
38. Portmann, S. & Lüthi, H.P. (2000) MOLEKEL. An Interactive Mol Graphics Tool. *CHIMIA* **54**, 766–770 (http://www.cscs.ch/molekel/)
39. Morokuma, K. (1971) Molecular orbital studies of hydrogen bonds: III. C=O…H_2O and C=O… $2H_2O$. *J. Chem. Phys.* **55**, 1236–1239.
40. Hehre, W.J., Radom, L., Schleyer, P.V.R. & Pople, J.A. (1986) *Ab Initio MO Theory*. Wiley, New York, USA.
41. Schmidt, M.W., Baldridge, K.K., Boatz, J.A., Elbert, S.T., Gordon, M.S., Jensen, J.J., Koseki, S., Matsunaga, N., Nguyen, K.A., Su, S., Windus, T.L., Dupuis, M. & Montgomery, J.A. (1993) GAMESS. *J. Comput. Chem.* **14**, 1347–1363.
42. Youshko, M., Shamolina, T., Guranda, D., Synev, A. & Svedas, V. (1998) Specific substrates for spectrophotometric determination of penicillin acylase activity. *Biokhimia* **63**, 1295–1300.
43. Alkema, W.B., de Vries, E., Floris, R. & Janssen, D.B. (2003) Kinetics of enzyme acylation and deacylation in penicillin acylase-catalyzed synthesis of β-lactam antibiotics. *Eur. J. Biochem.* **270**, 3675–3683.
44. Duggleby, H.J., Tolley, S.P., Hill, C.P., Dodson, E.J., Dodson, G. & Moody, P.C. (1995) Penicillin acylase has a single-amino-acid catalytic centre. *Nature* **373**, 264–268.
45. Done, S.H., Brannigan, J.A., Moody, P.C. & Hubbard, R.E. (1998) Ligand-induced conformational chnage in penicillin acylase. *J. Mol. Biol.* **284**, 463–475.
46. Alkema, W.B., Dijkhuis, A., de Vries, E. & Janssen, D. (2002) The role of hydrophobic active-site residues in substrate specificity and acyl transfer activity of penicillin acylase. *Eur. J. Biochem.* **269**, 2093–2100.
47. Morillas, M., McVey, C.E., Brannigan, J.A., Ladurner, A.G., Forney, L.J. & Virden, R. (2003) Mutations of penicillin acylase residue B71 extend substrate specificity by decreasing steric constrains for substrate binding. *Biochem. J.* **371**, 143–150.
48. Basso, A., Braiuca, P., Ebert, C., Gardossi, L., Linda, P. & Benedetti, F. (2002) GRID/tetrahedral intermediate computational approach to the study of selectivity of penicillin G acylase in amide bond synthesis. *Biochim. Biophys. Acta* **1601**, 85–92.
49. Carpenter, F.H. (1960) The free energy change in hydrolytic reactions: the non-ionized compound conventions. *J. Am. Chem. Soc.* **82**, 1111–1121.
50. Fersht, A. (2000) *Structure and mechanism in protein science*, 3rd edn, pp. 179–180. W.H. Freeman, New York, USA.
51. Lummer, K., Rieks, A., Galunsky, B. & Kasche, V. (1999) pH Dependence of penicillin amidase enentioselectivity for charged substrates. *Biochim. Biophys. Acta* **1433**, 327–334.